SIMPLIFIED RP-PERC PROCESS WITH TWO HIGH-TEMPERATURE STEPS

B. Fischer, M. Keil, P. Fath, E. Bucher
Universität Konstanz, Fachbereich Physik, Fach X916, 78457 Konstanz, Germany
Tel.: +49-7531-88-2082, Fax: +49-7531-88-3895
E-mail: bernhard.fischer@uni-konstanz.de

ABSTRACT: We compare the conventional RP-PERC process with a simplified process where the growth of an oxide to mask the emitter diffusion is replaced by a mesa-etching step. Thick positive photoresist is used to mask the mesa which is etched in an isotropic etching solution consisting of HNO_3 and NH_4F. Incomplete coverage of the pyramid tips with photoresist during the mesa etching results in Schottky-like shunts that limit the open circuit voltage while maintaining the short circuit current and good fill factor. We measure ideality factors below unity in the J_{SC}-V_{OC} characteristics and give an explanation which involves the dependence of the open circuit voltage on the series resistance. Different rear contact patterns are experimentally realised in solar cells and test structures which are characterised using photoconductance measurements under steady infrared light. The results are compared with calculations based on the three dimensional transport model of U. Rau.
Keywords: High-efficiency – 1: Simulation – 2: Characterisation –3

1. INTRODUCTION

The most successful silicon solar cell design is the PERC cell developed at the UNSW [1]. It features a regular inverted pyramid texture, double layer anti-reflection coating (ARC), two step emitter and a highly effective rear surface passivation and back surface reflector by a thermal oxide covered with aluminium. The base is contacted via an array of metal points with a boron diffused p^+-region underneath to reduce contact recombination and resistance. This is a highly sophisticated process leading to efficiencies above 24% and involves a large number of high temperature steps and accurately aligned photolithography steps.

A greatly simplified cell process which still leads to efficiencies well above 20% is the RP-PERC structure [2]. It replaces the inverted pyramid texture by a random pyramids, omits boron diffusion on the rear and the heavy phosphorus diffusion under the front contacts. The passivation oxide on the front also serves as a single layer ARC. This process involves two thermal oxidations and one diffusion, as well as two photolithography steps with relaxed alignment (ca. 200 µm).

The objective of this work was firstly to reproduce this process to have an adequate reference for comparison to novel concepts [3] which exhibit several additional difficulties. Also it is desirable to see the limitations to high lifetime processing in a rather industrial-like process environment (e.g. medium purity water with 10 MΩcm).

The usual RP-PERC process starts with growth of a thick thermal oxide which is opened on the front side of the active cell area, followed by the etching of random pyramids and emitter diffusion within the window.

Another aim was to replace these initial steps by firstly etching pyramids over the whole surface and a full area emitter diffusion. The unwanted diffused surface is then removed with an isotropic etch where photoresist is used to protect the final emitter. The advantages of this alternative are

- reduced risk to degrade the material quality during the high temperature oxidation
- isotropically etched pyramids on the rear produce a rough surface which can increase light absorption by almost 1 mA/cm² as calculated with the ray tracing simulation programme SUNRAYS [4]. Short circuit current might therefore increase unless increased recombination at the enlarged rear surface area compensates this gain.
- For the application of features of this process to multicrystalline Si the high-temperature steps should be minimised since most of these materials deteriorate in quality during these steps.

A first attempt to process conventional RP-PERC cells resulted in poor efficiencies below 18%. Their analysis revealed, that the weak points were an unsatisfactory rear surface recombination velocity (SRV) and poor bulk diffusion length L. In the following period we examined processing conditions and rear contact scheme by simulations and lifetime measurements as described in the following.

2. PROCESS CHARACTERISATION

The steady state photoconductance method [5] turned out to be an ideal technique to study the quality of oxidised silicon surfaces. However, rather than using the flash illumination originally supplied with the instrument we used an array of IR-LED's (875 nm) which is bright enough to produce a generation current density in silicon of 80 mA/cm². Since the generation profile is known the SRV can be calculated analytically from the measured photoconductance if the bulk lifetime is known (Here it was assumed to be 1ms).

It turned out that a true steady state measurement is essential when measuring oxide passivated surfaces by lifetime measurements since the effective lifetimes change when the samples are subjected to carrier injection. Figure 1 shows a typical example for the change in SRV measurements. The illumination with IR-LEDs also makes the relevant injection range accessible which is approx. $2 \cdot 10^{13}$ cm^{-3} for short circuit conditions, $5 \cdot 10^{13}$ cm^{-3} at the maximum power point and approx. $5 \cdot 10^{14}$ cm^{-3} under open circuit.

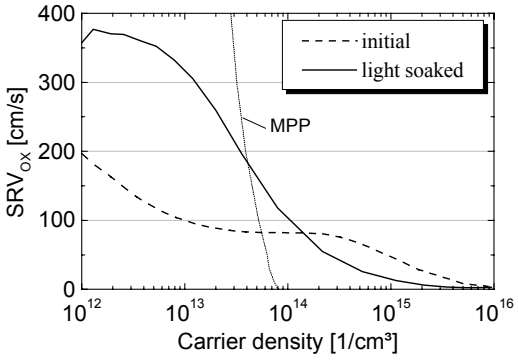

Figure 1: SRV of a passivation oxide measured by photoconductance. After a few tens of seconds under high carrier concentration (10^{15} cm^{-3}) the SRV degrades to a stable value representative for the solar cell performance.

We optimised the oxide growth conditions and rear contact pattern with this method, where it turned out that measurements are only meaningful after an 'Alneal', i.e. thermally evaporated Al, sintering at 400 °C and removal of the Al before measuring. This step greatly reduces oxide recombination and is an inherent part of the solar cell process when the Al back contact is formed.

Important results are that the SRV on an oxidized 0.5 Ωcm textured (random pyramids rounded by the mesa etch) was below 200 cm/s at $5 \cdot 10^{13}$ cm^{-3}, and not higher than on flat samples which measured 200-220 cm/s. The best sample with 2.5% points in 1600µm spacing was measured to SRV = 275 cm/s.

3. REAR METALLISATION PATTERN

In the PERC concept the carrier loss at the highly recombining metal contacts is kept acceptable by appropriate spacing and coverage fraction *f* of the point contacts. An optimum in efficiency has to be found since an increase in spreading resistance in the silicon adjacent to the metal contacts will oppose the effort to reduce recombination.

Unfortunately this is a three dimensional problem and can not be treated with PC1D (1-D) or DESSIS (2-D). Rau developed and describes in an excellent paper [6] an analytical simulation method by solving the transport equation for majority and minority carriers in Fourier space, which lends itself due to the periodicity of the point contacts in two dimensions.

We adapted his method, however, by neglecting the interaction between minority and majority carriers (Dember potential etc.) as well as assuming a constant potential at the junction we aimed at finding decoupled values of series resistance in the bulk and effective recombination velocities of the rear, instead of calculating IV-curves. The results can then be input into a one dimensional program such as PC1D together with the optical generation profile as determined with SUNRAYS to calculate the cell performance. Experience with these calculations led to the following useful results:

- It is a valid approach to express the effective rear SRV independently of bulk recombination. It is determined via the effective diffusion length L_{EFF} either by evaluating the short wavelength asymptote of 1/IQE or from the dark recombination current.
- The total rear SRV is within a few percent deviation the sum of contributions of the (homogeneous) oxide SRV_{OX} and the SRV_{MET} of the metal pattern alone (calculated with oxide recombination neglected).
- The recombination current into the infinitely recombining metal contact points the is limited by the supply with carriers from the bulk via diffusion. Therefore the SRV_{MET} scales on the whole linearly with the diffusion constant, which decreases with increasing doping concentration.

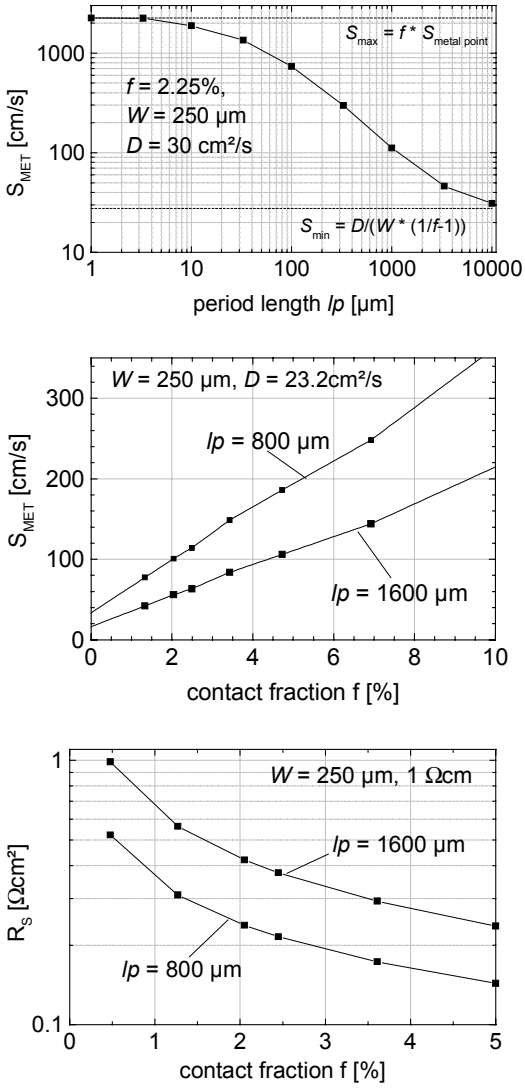

Figure 2: Surface recombination velocity of the point contact pattern as a function of period length *lp* (top) and fractional contact area *f* (center). Series resistance in the base for two period lengths as a function of contact fraction *f* (bottom).

Taking the simulation results together into a 1-dim. calculation we found that although current, voltage and fill factor will vary, the impact of the rear pattern on efficiency is very low. This is in agreement with the experimental results shown below.

4. CELL PROCESS

The material used was boron doped (100)-FZ-Si, 250 and 390 µm thick with resistivities from 0.3 and 0.5 Ωcm. The mesa-etched RP-PERC process starts with etching random pyramids in 3% NaOH with addition of isopropanol. After an RCA-cleaning the wafers receive a 130 Ω/sq POCl-diffusion at 835°C. After stripping the phosphorus glass in HF a thick layer of photoresist (AZ 4562) is spun onto the front side which is then structured to leave four 4cm² rectangles on the 5 x 5 cm² sample. The mesa is etched in 3 HNO_3 : 1 NH_4F (isotropic etch rate is approx. 3.5 µm/min) to remove the unwanted emitter. After stripping the resist and another RCA-clean a 109 nm thick passivation oxide is grown at 1000°C in oxygen with 3% HCl (i.e. its equivalent of Trans-LC) and annealed in Argon for 15 min. before slowly cooling down to 700°C. The diffusion and oxidation furnaces are cleaned before processing at 1100°C with HCl for two hours.

Photoresist is applied onto both sides and structured on front with a 10 µm finger-grid and the point pattern on the rear. After opening the oxide 50 nm of Ti, Pd and Ag are E-gun-evaporated onto the front and the excess metal removed in acetone. 1.3µm Al is then thermally evaporated onto the rear. The front grid is thickened by electroplating silver to get 20-25 µm wide fingers of 8-10 µm height. A 10 min anneal in forming gas at 400°C finishes the cell process. All cell processing is accompanied by a set of test structures for the lifetime measurements.

5. RESULTS AND LOSS ANALYSIS

Although having a slightly higher efficiency potential the mesa-etching process on textured samples is still inferior to the conventional mask-process. There appears to be a problem connected to a damaged emitter which leads to shunts, while the mesa-processed cells show short circuit currents higher than the mask references. These shunts, however, have a distinct Schottky like characteristic [7] rather than linear and therefore mainly reduce the open circuit voltage although many cells still show quite high fill factors. The photo masks used to expose the photoresist for the mesa etching was produced using a laser-printer [8]. These masks were probably not opaque enough so that some pyramid tips were opened. We are confident that with the use of a chromium photo mask this problem should be solved soon.

V_{OC} and J_{SC} for these defected cells do not correspond to a single effective diffusion length. From the injection dependence of the rear SRV this disagreement is usually the other way round, i.e. higher V_{OC} than to be expected from J_{SC}.

Table 1: Best cell results: mask RP: 0.3 Ωcm / 390 µm thick, mesa RP and mesa flat: 0.5 Ωcm / 250 µm thick

	J_{SC} (mA/cm²)	V_{OC} (mV)	fill factor (%)	η (%)
mask RP	37.2	671	81.8	20.4
mesa RP	37.4	648	80.6	19.5
mesa flat	32.5	672	82	17.9

For non-textured cells the mesa-etching proved to be a reliable process with results at least as good as the mask-process. We compared three different rectangular rear contact patterns in otherwise identical flat cells on 250 µm, 0.5 Ωcm FZ silicon. Table 2 shows the average results over 4 cells. As expected from the simulation the cell efficiency remains the same within the examined range of rear contact patterns. However, the choice of the pattern should fall to lower spacing and corresponding higher fill factors if Si-material of lower bulk diffusion length is used. On the other hand one should go to larger spacing if the rear oxide can be further improved.

Table 2: Comparison of 3 different rear contact patterns. Average over 4 cells, mesa-etched, no texture.

coverage & spacing	J_{SC} (mA/cm²)	V_{OC} (mV)	fill factor (%)	η (%)
2% 800µm	32.3	671	81.6	17.7
2.5% 1600µm	32.5	675	80.8	17.7
1.2% 1600µm	32.6	678	80.2	17.7

We observed for all solar cells which do not suffer from the shunting problem mentioned above that the illuminated JV-characteristics exhibits a negative slope in the low voltage range (i.e. < 400 mV) corresponding to a shunt resistance of about -10^4 Ωcm² . In figure 1 we see a change in the SRV after illumination from which a decrease in short circuit current with time should follow. This would appear as positive shunt which depends on the duration of illumination before the measurement or the voltage sweep rate. We could not observe such a dependence in JV measurements from which we conclude that these initially measured very low SRVs are only apparent. Most likely it is produced by some rearrangement of the occupation of the surface states leading to a change in surface conduction.

One likely explanation for the 'negative shunts' is the reduction of SRV_{OX} with increasing voltage (and therefore increasing carrier density). According to a simulation this would be expected if the SRV reduced by 15 cm/s in the range 0...300 mV.

Another effect we observed is that the ideality factor extracted from the J_{SC}-V_{OC} characteristics drops below unity for high voltages. We explain this by an impact of the series resistance on the open circuit voltage, an effect which is not commonly assumed and which is not expected from the diode equivalent circuit.

Recombination currents in the emitter split into two parts: the approx. 3% strongly recombining metallised region which is shadowed can be characterised by an emitter saturation current $J_{0E,MET}$ = 1 pA/cm². The oxide passivated and illuminated area we measured to $J_{OE,OX}$ = 20-40 fA/cm². The emitter is inherently connected with a larger series resistance than the metallised emitter which largely lies underneath the busbar. This inhomogeneity of the emitter recombination and illumination requires compensating 'lateral' currents to flow under open circuit conditions.

For low illumination these currents are small and hardly affected by the lateral resistance, thus the total J_{0E} is the area weighted sum. With increasing illumination the lowly recombining region is more and more screened by the larger series resistance which therefore can build up a higher voltage than the metallised region at which the voltage is measured.

This effect became obvious when some solar cells had many fingers interrupted where they should be connected to the busbar. By prolonged silver plating these interruptions could be bridged. In one instance the open circuit voltage increased then from 596 to 633 mV. An example for the J_{SC}-V_{OC} characteristics is shown in figure 5.

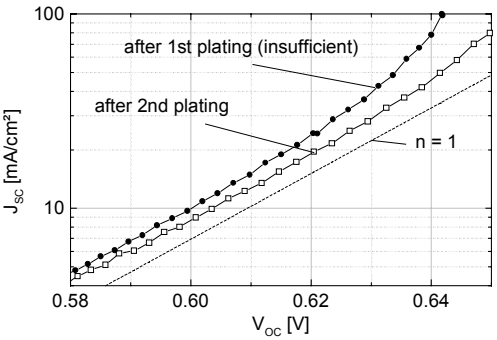

Figure 5: Ideality factor in J_{SC}-V_{OC} characteristics tends to go below unity for high voltages. Reducing the series resistance by re-plating Ag reduces the effect.

Loss analysis

The optical generation is difficult to measure directly and was therefore calculated using the programme SUNRAYS. With the 4.2% shading loss of the front grid the maximum gainable current ranges from 39.7 mA/cm² to 40.9 mA/cm² depending on cell thickness and rear surface roughness. About 0.9 mA/cm² more current may be generated if the rear is perfectly rough compared to ideally flat. The generation current for the thicker cells is about 0.2 mA/cm² higher.

Expressing the recombination currents in the different regions by their contribution to the diode saturation current J_0, we find:

2.6 % metallised emitter with a surface enlarged by a factor 1.7 by the texture amounts to 44 fA/cm² (J_{0E} = 1 pA/cm² for a metallised 100 Ω/sq emitter is taken from ref [9]). We measured the J_{0E} of the textured oxidised emitter to 37 fA/cm². From the typically achieved 670 mV for the textured 0.5 Ωcm solar cells the total J_0 is 180 fA/cm² of which about 80 fA/cm² is due to the emitter. At V_{OC} this leaves $J_{0,base}$ =100 fA/cm² for the base corresponding to an effective diffusion length of L_{EFF} = 840 µm.

The preferred rear contact pattern used in this work were points in 1.6 mm spacing covering 2.5% of the surface. The 3-D simulation for this pattern results in a contribution of the metal contacts of SRV_{MET} = 64 cm/s which is in good agreement with the measurements on the test structures which gave 200-220 cm/s for the oxide only and 275cm/s for the contact-patterned sample (at MPP). Recombination on the rear is therefore clearly dominated by the oxide. At V_{OC} the SRV for the contacted rear is reduced to 137 cm/s and the oxide alone to 60 cm/s (both on textured and flat).

The ratio of the currents recombining in the bulk and the rear surface can be expressed by

$$\frac{J_{BULK}+J_{REAR}}{J_{REAR}} = \cosh\left(\frac{W}{L}\right)+\frac{D}{L\,S}\sinh\left(\frac{W}{L}\right) \qquad (1)$$

with the cell thickness W = 250 µm, diffusion constant D = 23.2 cm²/s and S the SRV of the patterned rear.

Bulk diffusion length L was found to scatter in the lifetime measurements and IQE-analysis of the solar cells. We take L = 550 µm according to L_{EFF} of 840 µm at V_{OC} for S = 137 cm/s (L_{EFF} then reduces to 653 µm at MPP, corresponding to $J_{0,base}$ =132 fA/cm²). Using eqn. 1 we find that at V_{OC} 40 fA/cm² are due to rear surface recombination and 60 fA/cm² due to the bulk. At the MPP the rear recombination becomes dominant over volume with 72 fA/cm².

For the series resistance the 3-D simulation results in a contribution of the base of 0.19 Ωcm² (0.5Ωcm / 250 µm cells). Taking the front grid geometry (155µm² finger in 800 µm spacing) and a slightly enlarged Ag resistivity of 2 µΩcm the front grid contributes 0.25 Ωcm². The contact resistance on front (200 µΩcm²) and rear (150 µWcm²) contact was measured, giving rather small contributions of 4 mΩcm² and 6 mΩcm² to the series resistance. The measured total series resistance of the solar cells is well in accordance with the sum of these contributions of 0.45 Ωcm².

6. SUMMARY

The mesa etching process works perfectly for flat cells and is a useful simplification. On textured solar cells problems arise from imperfect coverage of the tips with photo resists which lead to non-classical shunts where the damaged emitter spots are metallised. Recombination and resistive losses calculated by 3-dimensional transport analysis are in good agreement with solar cell results and measurements on test structures by the IR-photoconductance method. The losses are well balanced with respect to the major compromises to be made between series resistance, shadowing and recombination losses.

ACKNOWLEDGEMENT

This work was supported within the JOULE 95 project by the European Commission under contract number JOR-CT 95-0030 (DG 12-WSME).

REFERENCES

[1] M.A.Green et al, IEEE Trans. El. Dev. 46 (10), (1999) 1940
[2] S.W. Glunz et al, 26th IEEE PVSC, Anaheim, (1997) 231
[3] B. Terheiden et al, *this conference*
[4] R. Brendel, Proc. 12th Euro. PVSEC, Amsterdam, (1994) 1339
[5] R.A. Sinton, A. Cuevas, Appl. Phys. Lett. 69 (17), (1996) 2510
[6] U. Rau, 12th Euro. PVSEC, Amsterdam, (1994) 1350
[7] M. Stocks, D. Macdonald, Proc. 16th Euro. PVSEC, Glasgow, (2000) 1671
[8] A. Hübner, C. Hampe, A. G. Aberle, Sol. En. Mat. 46, (1997) 67
[9] A. Cuevas et al, J. Appl. Phys. 80 (6), (1996) 3370